Antibody Therapeutics, 2020, Vol. 3, No. 4 ***227–236***
doi:10.1093/abt/tbaa022
Advance Access Publication on 9 November 2020

Research article

A novel antibody targeting TIM-3 resulting in receptor internalization for cancer immunotherapy

Zhihui Kuang†, Li Li†, Pan Zhang†, Bingliang Chen, Min Wu, Haiqing Ni, Shuai Yi, Jia Zou* and Junjian Liu*

Innovent Biologics (Suzhou) Co., Ltd., 168 Dongping Street, Suzhou Industrial Park, Suzhou 215123, Jiangsu, China

Received: September 9, 2020; Revised: October 28, 2020; Accepted: November 2, 2020

Abstract

Background: Strategies to reinvigorate exhausted T cells have achieved great efficacy in certain subpopulations of tumor patients. Blocking the antibodies that target programmed cell death protein 1 (PD-1) and cytotoxic T-lymphocyte-associated protein 4 induces durable responses in Hodgkin's lymphoma, melanoma, renal and lung cancers. T cell immunoglobulin mucin-3 (TIM-3) is another well-defined inhibitory receptor that is expressed in terminally differentiated Th1/Tc1 cells, which produces interferon gamma and cytotoxic molecules. It is also significantly expressed on forkhead box P3+ regulatory T cells and innate immune cells such as dendritic cells and macrophages.

Methods: By immunizing BALB/c mice with recombinant TIM-3 and screening of 20 000 hybridoma clones, we selected a monoclonal TIM-3-blocking antibody (IBI104), which shows great efficacy *in vitro* and *in vivo*.

Results: IBI104 blocks phosphatidylserine interaction with TIM-3 but does not interfere with the interaction of TIM-3 with galectin-9 in ELISA assays. However, *in vitro* administration of IBI104 induces the potent internalization of TIM-3 in activated T cells to the extent that it will shut down the entire TIM-3 mediated signaling regardless of the ligands. IBI104 shows potent anti-tumor efficacy when combined with anti-PD1 *in vivo*.

Conclusions: Our results suggest that IBI104 is a promising blocking antibody for TIM-3-mediated suppressive signaling and can serve as effective cancer immunotherapy, especially in combination with anti-PD1.

Statement of Significance: IBI104 was selected as the candidate, which showed a high binding affinity for human TIM-3. TIM-3 was reported to have distinct binding pockets for phosphatidylserine and galectin-9. We believe that our study makes a significant contribution to find a TIM-3 blocking antibody targeting phosphatidylserine binding pocket but induces the internalization of the whole molecule.

KEYWORDS: TIM-3; PtdSer-blocking antibody; IBI104; PD1; cancer immunotherapy

INTRODUCTION

Patients with advanced cancer benefit from checkpoint inhibition therapies such as anti-programmed cell death protein 1 (PD1) and anti-cytotoxic T-lymphocyte-associated protein (CTLA4)-based immunotherapy. However, only a proportion of such patients respond to monotherapy. Additionally, in some tumor types, a large proportion of cancers in patients are refractory to CTLA4 and PD-1 blockade, such as colorectal cancer and gastric cancer. Therefore, there is an urgent need to identify other co-inhibitory receptors that can either act in concert with PD-1 or CTLA4 to suppress T cell responses, or play a major negative role in the regulation of immune responses

*To whom correspondence should be addressed. Jia Zou and Junjian Liu. Email: jia.zou@innoventbio.com and junjian.liu@innoventbio.com

†These authors contributed equally to this work.

in some tumor types. TIM-3, a well-documented member of the T cell immunoglobulin and mucin domain (TIM) superfamily, is another promising candidate for cancer immunotherapy. Pre-clinical studies have shown that blocking the mouse TIM-3 with antibodies can reduce mouse tumor burden [1, 2]. An anti-human TIM-3-blocking antibody has also been shown to enhance the New York esophageal squamous cell carcinoma-1 (NY-ESO1) specific cluster of differentiation (CD8+) T cell responses in advanced melanoma patients [3]. More interestingly, TIM-3 was reported to be upregulated in anti-PD-1 therapy-resistant cancer patients [4, 5]. These pre-clinical data and clinical observations suggest that TIM-3 may play a critical role in suppressing anti-tumor responses and is a great impetus for the development of anti-human TIM-3 antibodies for clinical applications.

TIM-3 has multiple ligands. It was first reported that the C-type lectin, galectin-9, can bind to TIM-3 [6]. A second ligand was revealed by studying the crystal structure of TIM-3, which shows a unique binding cleft that can interact with phosphatidylserine (PtdSer) [7, 8]. Later, two other molecules, high-mobility group protein 1 (HMGB1) [9] and carcinoembryonic antigen-related cell adhesion molecule 1 (CEACAM1) [10], have also been implicated as TIM-3 ligands. Although TIM-3 has multiple ligands, the crystal structure suggests that PtdSer, CEACAM1 and HMGB1 binding sites depend on hydrophobic residues in the FGCC' loop [9–11]. In contrast, the galectin-9 binding sites are positioned at the opposite FGCC' site and are distinct. These distinct ligand-binding sites make it challenging to completely block TIM-3 signaling using a single antibody.

Here, we describe the generation of a humanized anti-TIM-3 monoclonal antibody (mAb) IBI104. IBI104 was found to block the binding of PtdSer to TIM-3. As expected, IBI104 did not interfere with galactin-9 binding to TIM-3 in enzyme-linked immunosorbent assay (ELISA). Interestingly, binding of IBI104 to the CEACAM1/PtdSer/HMGB1 binding sites, but not the galectin-9 binding sites, induces the strong internalization of TIM-3 in activated human peripheral blood mononuclear cells (PBMCs). The impact of antibody-induced internalization is a complete blockade of TIM-3 signaling induced by all ligands. As a result, IBI104 displayed promising anti-tumor activity in combination with PD-1 mAbs in mouse tumor models.

RESULTS

Binding affinity and specificity of IBI104 in blocking the PtdSer-TIM-3 interaction

An anti-TIM-3 mAb was developed using hybridoma technology, for which BALB/c mice were immunized with recombinant TIM-3. A total of 20 000 hybridoma clones were harvested, from which 11 clones were only reactive to TIM-3. After several rounds of screening based on binding affinity and specificity, a TIM-3-blocking antibody clone IBI104 was selected as a lead molecule for detailed characterization.

First, we used surface plasmon resonance to determine the binding affinity of IBI104 to human and cynomolgus TIM-3. The dissociation constant (K_D) of IBI104 was 3.768 nM against human-TIM-3 and 10.4 nM against Cyno-TIM-3 (Fig. 1A and B). These results were confirmed using a cell-based binding assay using Chinese hamster ovary (CHO-S) cells stably overexpressing either human-TIM-3 or Cyno-TIM-3. The half maximal effective concentration (EC_{50}) of IBI104 binding to CHO-S-hTIM-3 was 1.355 nM, and the EC_{50} was 1.335 nM when binding to CHO-S-Cyno-TIM-3 (Fig. 1C and D). Thus, IBI104 has a high affinity for both human- and Cyno-TIM-3. We also examined the non-specific binding of IBI104. The polyclonal antibody in human serum is coupled to HiTrap NHS-activated column, and then the residence time of the candidate antibody on the column is measured to detect the non-specific binding of the antibody. The longer the residence time of the antibody indicates that the antibody may non-specifically bind to substances in the serum. In this study, we have a positive control monoclonal antibody, which we have found to have non-specific binding, and a negative control antibody against human TNF-alpha, which is a known antibody with very high specificity. As shown in Supplementary Fig. 1, we found that the peak of IBI104 and residence time is quite similar as negative control and distinct from positive control mAb which has known non-specificity.

Next, we examined whether IBI104 can bind to primary human T cells after activation *in vitro*. It is known that upon T cell receptor (TCR) activation, human T cells can upregulate endogenous TIM-3. The results showed that IBI104 can effectively bind to these TIM-3+ T cells *in vitro*, with an EC_{50} of 0.07745 nM (Fig. 1E). To determine which ligand interaction can be blocked by IBI104 after binding, we conducted a cell-based blocking assay using IBI104, biotin-PtdSer and the CHO-S-hTIM-3 stable cell line. We found that the binding of PtdSer can be effectively blocked by IBI104 with a half maximal inhibitory concentration (IC_{50}) of 9.374 nM (Fig. 1F).

Functional characterization of IBI104 *in vitro*

We next sought to address whether IBI104 can have a functional impact on *in vitro*-activated human PBMCs. We set up a mixed lymphocyte reaction (MLR) assay using human PBMCs from different healthy donors. Interleukin 2 (IL-2) and interferon gamma (IFNγ) release was measured to indicate the activation of PBMCs. Results showed that IBI104 alone cannot enhance IL-2 and IFNγ production, whereas an anti-PD1 (IBI308) antibody significantly increased both cytokine levels in the cell culture supernatant (Fig. 2A and B). The combination of IBI104 with anti-PD1 antibody further enhanced IL-2 production at certain concentrations (Fig. 2A), indicating that blocking TIM-3 along with PD-1 can maximize immune cell reinvigoration *in vitro*. Since T cells comprise a major population in the PBMC culture, we intended to specifically examine natural killer (NK) cell responses *in vitro* in human PBMCs. We mixed K562 cells with human PBMCs to activate only NK cell populations *in vitro*. Since K562 cells scarcely express major histocompatibility (MHC) class I molecules on their cell membrane, they are highly sensitive to NK cells. Co-culturing K562 cells with PBMCs

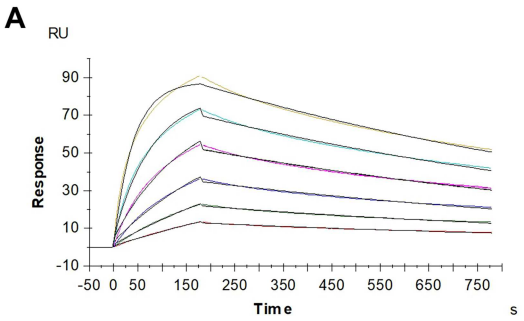

K_D (M)	ka (1/Ms)	kd (1/s)
3.768E-9	2.390E+5	9.005E-4

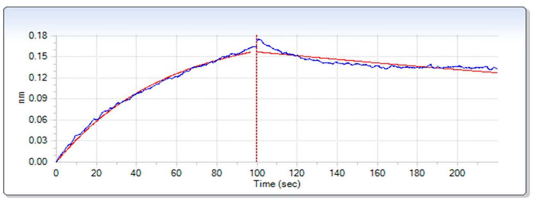

K_D (M)	ka (1/Ms)	kd (1/s)
1.04E-8	1.69E+5	1.76E-3

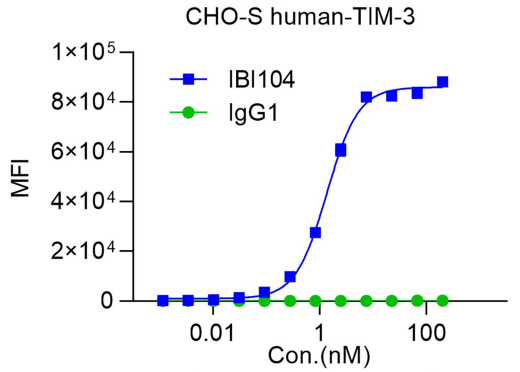

	IBI104
EC50	1.355

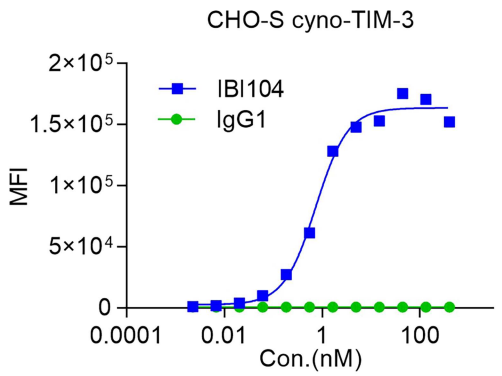

	IBI104
EC50	0.7469

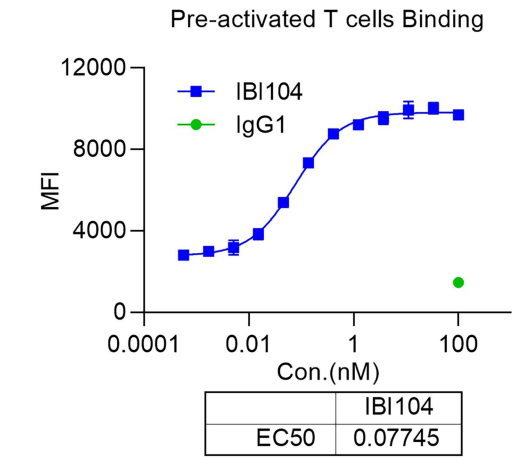

	IBI104
EC50	0.07745

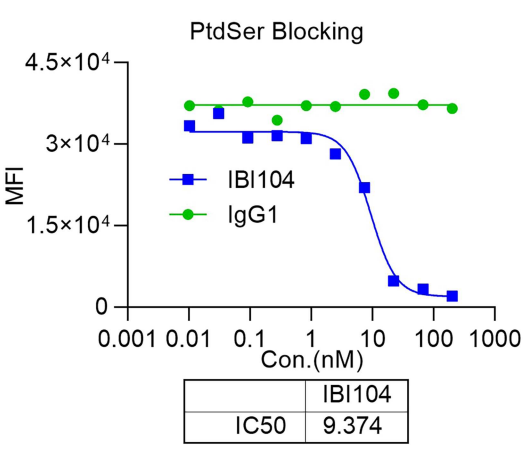

	IBI104
IC50	9.374

Figure 1. Characterization of IBI104 by antigen binding/blocking. (A) Binding affinity of IBI104 to soluble human-TIM-3 by SPR. IBI104 was used as 2 ug/mL, Tim-3 antigen was diluted for six 2-fold dilutions from 100 nM. KD, binding dissociation equilibrium constant; Ka, kinetic association rate; Kd, kinetic dissociation rate. (B) Binding affinity of IBI104 to soluble Cyno-TIM-3 by BLI. IBI104 was used as 2 ug/mL, Tim-3 antigen was diluted for six 2-fold dilutions from 100 nM. KD, binding dissociation equilibrium constant; Ka, kinetic association rate; Kd, kinetic dissociation rate. (C, D) Graphs showing cell binding of IBI104 to Human-TIM-3-expressing CHO-S and cyno-TIM-3 expressing CHO-S. IgG1 is the isotype control. (E) Binding of pre-activated T cells. (F) The PtdSer-blocking ability of IBI104 was analyzed in L363 cells. Apoptosis was induced in L363 by using H2O2. All experiments were repeated in at least two independent sets showing representative results.

containing NK cells resulted in NK cell activation and degranulation. Flow cytometry analysis showed the expression of NKG2D, which was an indication that NK cell activation had markedly increased after the TIM-3 blockade by IBI104 (Fig. 2C). Consistent with this, CD107a expression on NK cells indicating their degranulation was also upregulated upon IBI104 addition in a dose-dependent manner (Fig. 2D). Taken together, our results indicated that IBI104 alone can enhance NK cell activation *in vitro*. It has been reported that TIM-3-mediated functional exhaustion can be mediated by distinct mechanisms, including the FGCC' loop where PtdSer, CEACAM1 and HMGB1 bind and a distinct galactin-9 binding pockets. IBI104 was shown to block PtdSer-binding (Fig. 1F); when examining the exact mechanism of the signaling pathway by which IBI104 reinvigorates T cell and NK cell activation, we were surprised to find that IBI104 elicits TIM-3 internalization (Fig. 2E). This potentially blocks interactions with ligands other than those of PtdSer-induced negative signaling in T and NK cells. To examine whether antibody-induced internalization is a special attribute of IBI104, we further carried out TIM3 internalization assay using TSR-022, developed by Tesaro in collaboration with AnaptysBio, and now in a Phase 1 clinical trial. We found that TSR-022 can also mediate TIM3 internalization but the EC50 is about 3-fold higher (Fig. 2F), which means that IBI104 induced stronger internalization than TSR-022.

Anti-tumor efficacy of IBI104 in TIM-3-humanized mouse models

Considering that IBI104 can efficiently bind to humanized Tim-3 (hTIM-3) and Cyno-TIM-3 but not murine-TIM-3, we evaluated the *in vivo* efficacy of this antibody in humanized TIM-3 knock-in (hTIM-3-KI) mice. First, we examined the tumor-infiltrating lymphocytes in established subcutaneous MC38 tumors in hTIM-3-KI mice. Flow cytometry analysis showed that in both CD4+ and CD8+ T cells, TIM-3 was predominantly expressed on a subset of PD-1+ T cells but was not readily detected on PD-1-negative T cells, indicating that TIM-3 may be a late exhaustion marker, whereas PD-1 is an early exhaustion marker (Fig. 3A). We did not observe the significant expression of either TIM-3 or PD-1 on tumor-infiltrating NK cells (data not shown), consistent with a recent report showing that TIM-3 and PD-1 can only be significantly induced on NK cells with MHC-I knockout tumor cells *in vivo* [12]. Next, we determined the *in vivo* efficacy of tumor growth control using anti-TIM-3, anti-PD1 or combination therapies in the MC38 model. Results showed that IBI104 alone did not affect MC38 growth in hTIM-3-KI mice, whereas anti-PD1 alone reduced tumor burden by half (Fig. 3B and C). More importantly, the combination of IBI104 and anti-PD1 further suppressed MC38 growth (Fig. 3B and C), indicating that TIM-3 blockade can be used as a combination therapy with anti-PD-1 and potentially other checkpoint inhibitors. By measuring the body weight of tumor-bearing mice in the treatment groups, we did not find any reduction in body weight in the IBI104 or IBI104 + anti-PD-1 combination groups (Fig. 3D), indicating that anti-TIM-3 was more effective in immunotherapy without inducing additional immune-related adverse effects. By analyzing tumor-infiltrating NK cell percentages, we did not find a statistically significant increase in IBI104-treated mice, but the NK cell percentage in the combination group was significantly higher than that in the anti-PD1 monotherapy group (Fig. 3E). Consistent with the high T cell expression of both PD-1 and TIM-3 in the MC38 model as shown in Fig. 3A, we found a significant increase in both CD4+ and CD8+ T cell proliferation after anti-PD1 treatment, and IBI104 further increased CD4+ T cell proliferation, as indicated by Ki67 staining (Fig. 3F). Next, we examined the infiltration of Tregs in the TILs and we found that anti-PD-1 treatment or IBI104 alone or in combination does not increase this ratio (Supplementary Fig. 2A). Thus, we conclude that IBI104 does not exert its therapeutic effect through Treg. In the meantime, we observed no change in CD8/CD4 ratio in the TIL after IBI104 treatment either (Supplementary Fig. 2B). Finally, we also analyzed memory T cell subsets in the spleen of tumor bearing mice after treatment; in particular, we looked into effector memory T cells (CD62L-CD44+), central memory T cells (CD62L + CD44+) or total T effector cells (CD44+) or total naïve T cells (CD44-CD62L+). We found that there is significant increase of Tem, Teff cell populations in the anti-PD-1-treated spleens, whereas Tcm and Tn cells were decreased (Supplementary Fig. 3A–D). This indicates that anti-PD-1 indeed induced an activated T cell phenotype in the host. In contrast, we did not observe additional effect of IBI104 treatment (Supplementary Fig. 3A–D). This reflects a minor role of inhibiting TIM3 signal in overall T cell activation *in vivo* in this tumor model.

Taken together, our *in vivo* pre-clinical mouse tumor model showed that blocking TIM-3 alone has a limited effect on tumor control, but it can significantly enhance the therapeutic effects of anti-PD1 immunotherapy.

Pharmacokinetic profile of IBI104

The pharmacokinetics (PK) of IBI104 were evaluated in BALB/c mice following a single I.V. injection at a single dose of 10 mg/kg. The plasma drug concentrations of uninjected BALB/c mice were below the detection limit, and after a single injection, plasma drug concentrations increased to ~200 μg/mL (Fig. 4). All detailed PK parameters are listed in Table 1. No gender differences in the major PK parameters were observed (data not shown).

DISCUSSION

Here, we describe a novel and potent humanized, blocking antibody that targets human- and cyno-TIM-3 for potential application in cancer immunotherapy. The existence of four reported ligands and two distinct ligand-binding interfaces has raised a major challenge not only for understanding TIM-3 biology but also for developing a complete blocking antibody. Given the established role of TIM-3 as a checkpoint inhibitor similar to PD-1 and CTLA4, it is of great importance to develop antibodies that can fully block this pathway to add new tools for cancer immunotherapy. Interaction of TIM-3 with PtdSer

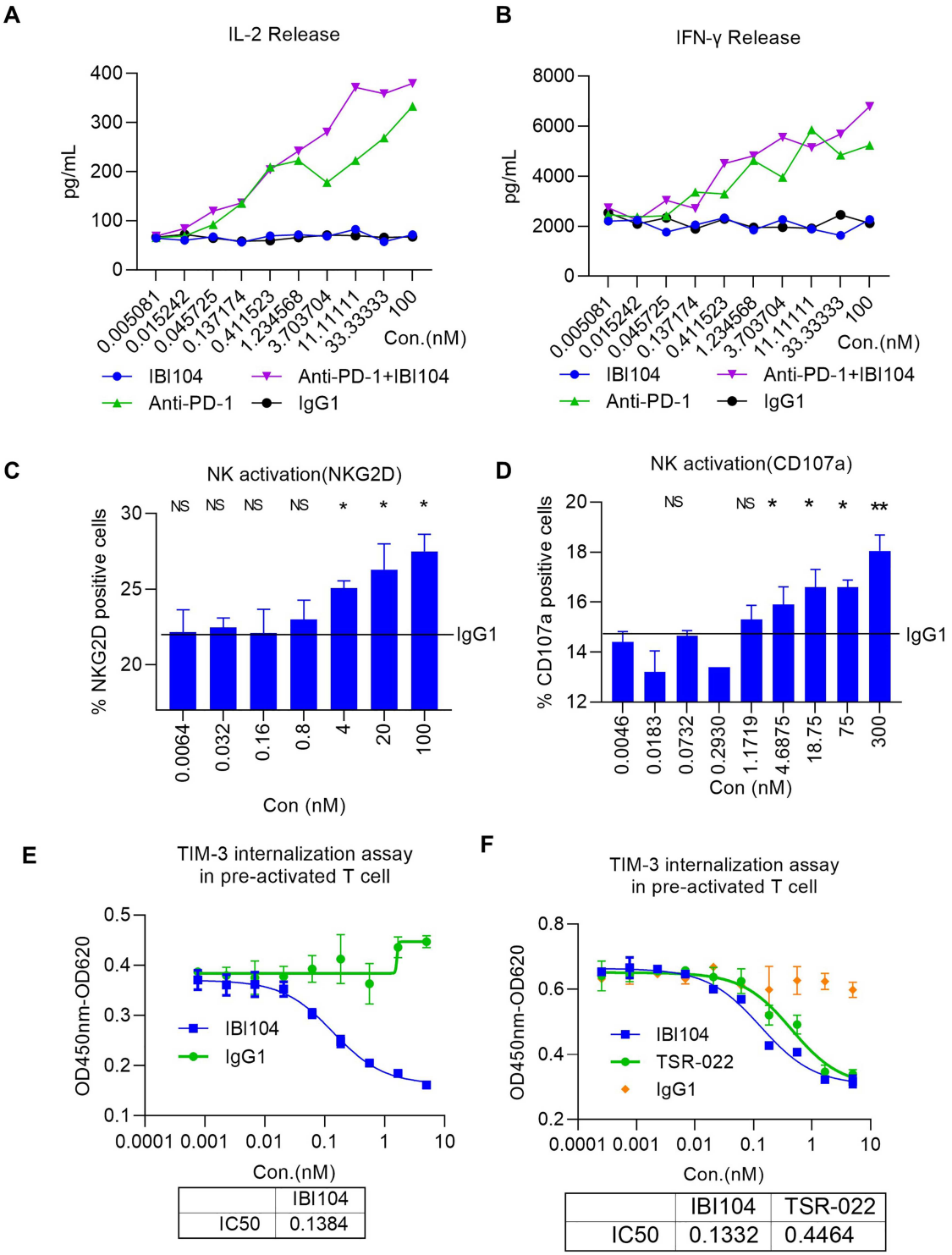

Figure 2. Characterization of IBI104 in the *in vitro* cell-based assays. (A, B) In an MLR assay, matured DCs and CD4 T cells were co-cultured in different concentrations of antibodies for 96 h. (A) IL-2 and (B) IFNγ were analyzed using ELISA. (C, D) In an NK activation assay, NK and K562 cells were co-cultured; Graphs show different concentrations of antibodies for 4 h. (C) NKG2D and (D) CD107a were analyzed using flow cytometry. (E) In the TIM-3 internalization assay, pre-activated T cells were plated onto a flat-bottom dish for 3 days at 37°C; cell suspension included Fab-ZAP along with mAb. The determination of cell viabilities was performed using the Cell Counting Kit-8. All experiments were repeated in at least two independent sets showing representative results. (F) TIM-3 internalization assay in pre-activated T cells was performed using IBI104 and TSR-022 monoclonal antibodies for 3 days as in (E).

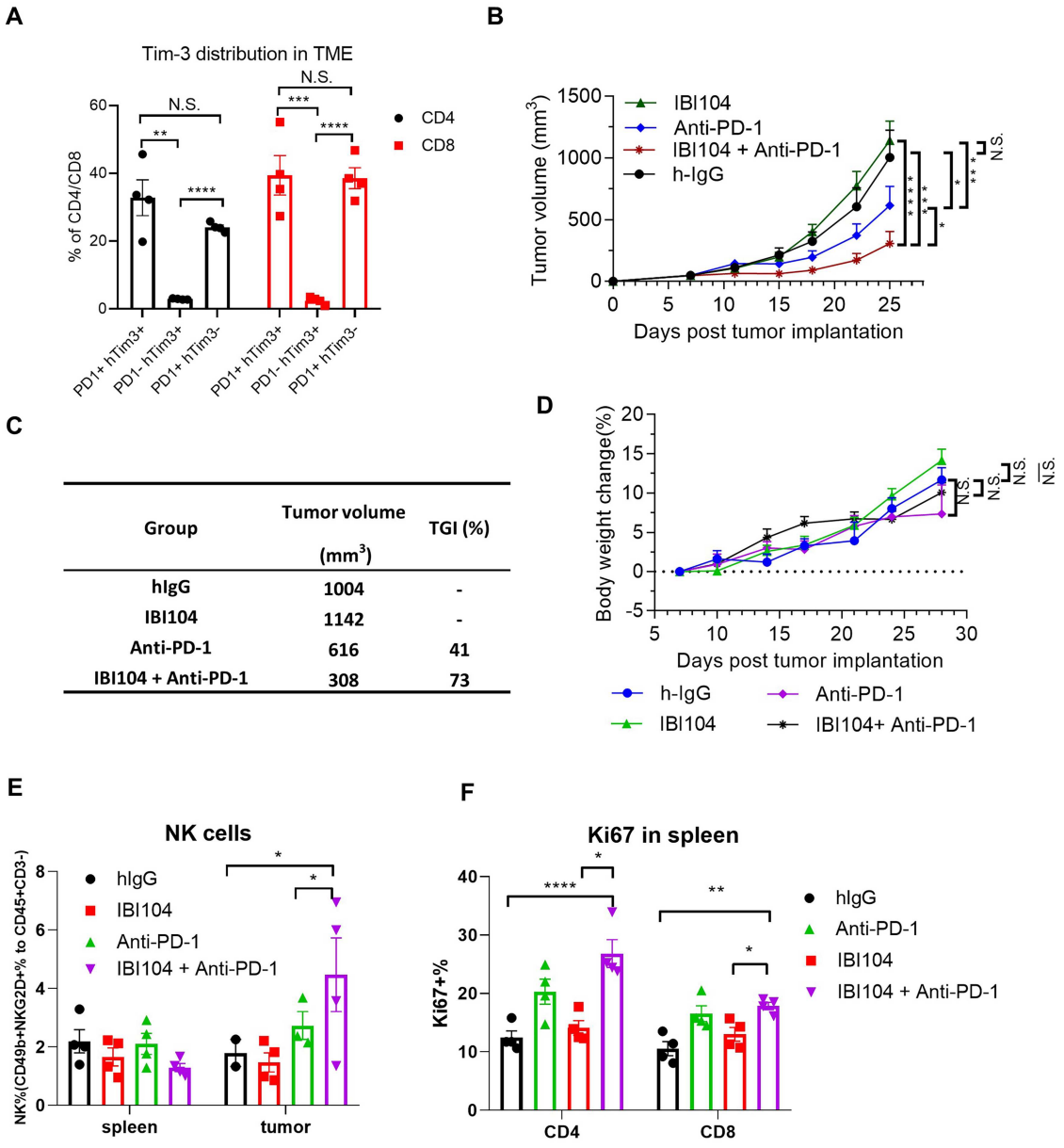

Group	Tumor volume (mm^3)	TGI (%)
hIgG	1004	-
IBI104	1142	-
Anti-PD-1	616	41
IBI104 + Anti-PD-1	308	73

Figure 3. IBI104 showed potent anti-tumor activity in TIM-3 knock-in mouse bearing MC-38 tumors. (A) Percentage of mouse PD-1 and human TIM3 positive cells in CD4 and CD8 cells of the TILs from MC38 tumor bearing h-TIM3-KI mice at day 25. (B) IBI104, Anti-PD-1 and IgG1 anti-tumor effects were evaluated in TIM-3 knock-in mouse models seeded by MC38 cells. $N = 7$; Bars represent mean ± SE. (C) Tumor volume and tumor growth inhibition in mice on day 25 after tumor cell implantation. (D) Animal body weights were measured during the course of the experiments. (E) NK cell percentage in the spleen and tumor of indicated groups by FACS. (F) Ki67 percentage in the spleen of indicated groups by FACS.

Table 1. Pharmacokinetic profile of IBI104 in BALB/c mice

Group	$t_{1/2}$ h	C_{max} μg/mL	$AUC_{0\text{-inf}}$ μg/mL*h	CI (μg)/(μg/mL)/h
IBI104	119	208	23175	0.008

has been reported to induce IL-10 in T cells [13]. The complete shutdown of galectin-9/TIM-3 interaction is also critical because galectin-9 has been reported to mediate TIM-3 incorporation into immunological synapses and co-localize with CD45 phosphatases to dampen TCR signaling [14]. The *in vivo* administration of galectin-9 was found to dampen Th1-type immune responses [6]. CEACAM1-TIM-3 and galectin-9 TIM-3 have shown similar downstream signaling in which the Bat3 protein is released from the cytoplasmic tail of TIM-3 [10, 15]. Taken together, it is

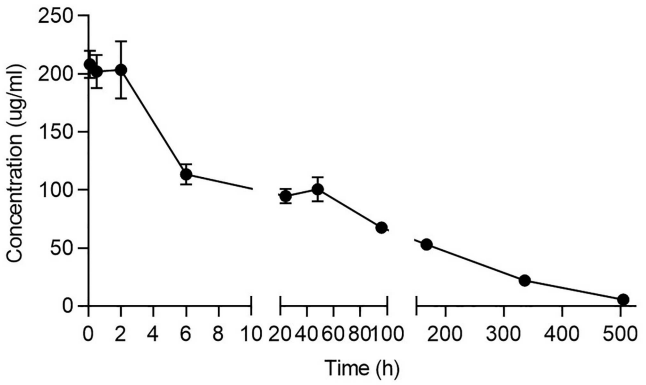

Figure 4. PK profile of IBI104 in BALB/c mice. Drug concentration-time curves of BALB/c mice after successive I.V. administrations of 10 mg/kg IBI104 ($n = 3$).

critical to block all of these ligand-TIM-3 interactions to prevent an inhibitory signal from TIM-3. We have achieved this goal by developing a potent blocking antibody that binds to the critical binding site of PtdSer, which induces a strong internalization of TIM-3 and results in a complete signal blockade. The exact mechanism of action regarding how IBI104 binds to CEACAM1/PtdSer/HMGB1-binding sites needs to be determined by studying the crystal structure.

In mouse tumor models, we observed that a fraction of PD-1+ T cells expressed TIM-3. This indicates that TIM-3 can provide another layer of T cell exhaustion in a hierarchical manner during tumor development after PD-1. TIM-3+ PD1+ T cells may represent a 'deeper' state of dysfunction compared with PD1 single positive T cells. Thus, functional reinvigoration by PD-1-blocking agents may not be sufficient to restore the ability of double positive T cells to proliferate and kill tumor cells. The application of TIM-3-blocking agents such as IBI104 demonstrated synergistic effects in restoring T cell function. In the mouse tumor models studied, we did not detect a significant amount of TIM-3 expression on tumor-infiltrating NK cells, which could be the main reason why monotherapy with IBI104 failed to show any efficacy in pre-clinical models; however, a few recent human studies have reported TIM-3 expression [16] as well as co-expression with PD-1 [17] on NK cells in cancer patients. It was reported that NK cells from patients with advanced melanoma express high levels of TIM-3, which is associated with poor prognosis. The *in vitro* treatment of such TIM-3+ NK cells can reverse their exhaustion phenotype [16]. Additionally, the highest TIM-3 expression is found on the surface of NK cells in human PBMCs, especially on mature $CD56^{dim}CD16^{+}$ subsets [18]. We speculate that under such circumstances, monotherapy with anti-TIM-3 can elicit a promising immune response, since our *in vitro* analysis showed that IBI104 alone can greatly enhance NK cell activation and degranulation. We did notice that in one point, our *in vitro* assay cannot fully explain our *in vivo* observation. The MLR assay using DCs and T cells *in vitro*, IBI104 did not enhance IFN-g production and only slightly increase IL-2 production even under combinational conditions. In contrast, in the same experiment, blocking PD-1 can greatly increase both T-cell-related cytokines. Interestingly, IBI104 can alter NK cell activation status *in vitro* as illustrated in Fig. 2C and D. But *in vivo* results showed that IBI104 alone cannot enhance antitumor activity, meanwhile, we observed not only NK cell activation but also T cell activation enhancement under combinational therapy which cannot be simply explained by *in vitro* assay results. We speculate that *in vivo* activation of NK cells in the context of T cell exhaustion release by PD-1 blockade can further enhance T cell anti-tumor function. There was a report showing that NK cells are main source of Flt-3 L [19], a cytokine which is critical for DC expansion and resulted in better T cell activation.

Apart from T cell and NK cells, which are two major tumoricidal immune cell populations that can be targeted by anti-TIM-3 antibody, other cell types such as dendritic cells (DCs) and macrophages were also found to show surface TIM-3 expression [9, 20, 21]. It was reported that TIM-3 expression on macrophages or monocytes downregulates IL-12 expression [21]. More importantly, the PtdSer-TIM-3 interaction on macrophages is critical for the engulfment of apoptotic cells. Such clearance of apoptotic bodies by phagocytes *in vivo* is important for maintaining immune tolerance. However, TIM1 [22] and TIM4 [23, 24] can also mediate such phagocytosis by binding to PtdSer, and whether the loss of TIM-3 has a significant impact on apoptotic cell clearance needs further investigation. Finally, TIM3 is also expressed on DCs and other myeloid cells such as macrophages and neutrophils. It was shown that in DCs, TIM-3 interaction with HMGB1 prevented the localization of nucleic acids into endosomal vesicles and in turn dampen DNA mediated anti-tumor responses [25]. We thought this mechanism is predominantly critical in the circumstances for inducing antitumor immunity in conjunction with DNA vaccines. Whether TIM3 expressed on DCs will contribute significantly in normal tumor growth models remain to be studied by using DC specific cre in combination with floxed TIM3 allele. Due to the lack of this valuable genetic mouse model, a definitive answer to this question is still lacking but warrant further study.

Taken together, the *in vivo* efficacy of anti-TIM-3 antibody in cancer immunotherapy can be partially attributed to the role of TIM-3 in accessory cells such as DCs and macrophages. Therefore, further studies are required to explain the effect of TIM-3 signaling blockage on different cell subsets by using TIM-3 conditional knockout mouse models.

In summary, this study reports a potent TIM-3-blocking antibody (IBI104) with detailed characterization of its binding and blocking properties, PK and *in vivo* efficacy. The ability of IBI104 to induce TIM-3 internalization, which resulted in a complete signal blockade, makes it a promising candidate for clinical development in cancer immunotherapy.

MATERIALS AND METHODS

Animals

The hTIM-3-KI mice were purchased from the Shanghai Model Organisms Center, Inc., Shanghai, China. BALB/c

mice were purchased from the Beijing Vital River Laboratory Animal Technology Co., China. All mice were maintained under pathogen-free conditions in the Experimental Animal Center of Innovent Biologics Co., Ltd. (Suzhou, China). All mouse experiments were approved by the Animal Use and Care Committee of Innovent Biologics.

Cell line construction

CHO-S stable cell lines expressing exogenous human or cynomolgus TIM-3 were generated according to the manufacturer's instructions using the Freedom CHO-S Kit (Invitrogen, Carlsbad, CA, USA).

Antibody generation

BALB/c mice (Beijing Vital River Laboratory, China) were immunized with a recombinant human Tim3 protein. The antibody immune response was monitored by ELISA. When a desired immune response was achieved, splenocytes were harvested and fused with mouse myeloma cells SP2/0 to preserve their viability and form hybridoma cell lines. The electrofusion was performed according to manufacturer's guidance (ECM2001, BTX, USA). The cells were plated into 96-well plates; after 7–10 days incubation, the hybridoma supernatants were screened and selected to identify cell lines that produce Tim3-specific antibodies. Using this technique, several anti-Tim3 antibodies were obtained.

The antibody was purified in-house (Innovent Biologics Co., Ltd., Suzhou, China) from HEK293 cells with either transient or stable expression unless indicated otherwise.

Cell culture

Human PBMCs (AllCells, Alameda, CA, USA) were cultured in AIM V® Medium CTS (Gibco, USA). K562 cells were cultured in RPMI 1640 medium (Gibco, USA) with 10% fetal bovine serum and 1% penicillin–streptomycin (Gibco, USA).

Enzyme-linked immunosorbent assay

Detection of IL-2 and IFNγ was conducted according to the manufacturer's protocol (eBioscience, Thermo Fisher Scientific, Waltham, MA, USA). Optical density (OD) measurements were obtained using a Multiskan FC system (Thermo Fisher Scientific, USA).

Affinity and specificity studies

Antibody affinities were determined using biolayer interferometry (ForteBio, Fremont, CA, USA). The experimental antibody was biotinylated using the EZ-Link Sulfo-NHS-LC-Biotin kit (Thermo Fisher Scientific, USA) and loaded onto SA–Streptavidin biosensors at the indicated concentrations. After washing, the sensors were dipped into a buffer containing antigen at the indicated concentrations and then dissociated in a sample dilution (SD) buffer (SD buffer: 50 mL PBS + 0.1% bovine serum albumin (BSA) + 0.05% Tween-20). Data analysis was performed using the ForteBio software (Data Analysis 7.0). Surface plasmon resonance analysis was carried out using CM5 sensor chips (GE Healthcare, Chicago, IL, USA) to measure the affinity kinetics between IBI104 and PtdSer.

Internalization assay

Human CD4+ T cells isolated from PBMCs using the EasySepTM human CD4+ T enrichment kit (STEMCELL Technologies, Vancouver, Canada) were pre-stimulated with DynabeadsTM CD3/CD28 (Gibco, USA). Four days later, pre-stimulated T cells at a density of 2×10^5 cells per well were co-cultured with serially diluted IBI104 and FabZAP(ADVANCED). Three days later, cell viability was determined using the cell counting Kit-8 (Dojindo, USA).

NK activation assay

Human NK cells (AllCells, Alameda, CA, USA) and K562 (ATCC, Manassas, USA) were co-cultured in the presence of titrated antibodies for 5 h. The percentage of NKG2D and CD107 was measured using flow cytometry (BD Biosciences, USA).

Flow cytometry

Cells were first incubated with an Fc-blocking Ab (2.4G2) and then labeled with fluorescently labeled mAbs for 30 min in phosphate buffered saline (PBS) with 1% BSA. The stained cells were collected on an Accuri C6 system (BD Biosciences, San Jose, CA, USA) or a BD FACSCelesta flow cytometer (BD Biosciences, USA). Data analysis was performed using FlowJo software (FlowJo, LLC, Ashland, OR, USA).

MLR assay

Monocyte-derived DCs were isolated from adherent cells of 5-day-old cultures of PBMCs from healthy donors. DCs were further differentiated *in vitro* for 2 days in the presence of recombinant human tumor necrosis factor-alpha (1000 U/mL), IL-1β (5 ng/mL), IL-6 (10 ng/mL) and Prostaglandin E_2 (1 μM). $CD4^+$ T cells were isolated from the PBMCs of a different donor. $CD4^+$ T cells and DCs were co-cultured in the presence of titrated antibodies ranging from 0.005081 to 100 nM for 3 days. The levels of IL-2 and IFNγ in the culture supernatant were measured using ELISA.

MC38 tumor model in hTIM-3-KI mice

MC38 cells (1×10^6 cells in PBS) were inoculated subcutaneously into the right flank of hTIM-3-KI female mice. On day 6, mice were randomized into 7 groups ($N = 7$) with an average tumor volume of ~100 mm^3. On days 6, 9, 12 and 16 post-tumor inoculation, mice were injected in the peritoneum with the indicated antibodies at 10 mg/kg. Tumor volume and body weight were measured twice a week, and the mice were euthanized when tumor volume reached 2000 mm^3, or the percentage of body weight loss exceeded 20%.

Dissociation of tumor-infiltrating lymphocytes for flow cytometry analysis

Tumors were excised, minced and digested for 45 min with gentle shaking at 37°C in Hanks' balanced salt solution containing 7 mg/mL collagenase D and 200 μg/mL DNase-I (Roche). Single-cell suspensions were subjected to centrifugation using a 40:80 percoll (GE) gradient. The separated cell layers in the middle were collected for further analysis.

Antibodies used for flow cytometry

The following antibodies were used: α-CD45 (BioLegend, Cat. #:103149), α-CD8 (Invitrogen, Cat. #:45–0081-80), α-CD4 (Invitrogen, Cat. #:25–0042-82), α-CD3 (BioLegend, Cat. #:100341), α-CD3 (BioLegend, Cat. #:100206), α-CD107a (BioLegend, Cat. #:328626), α-CD56 (BioLegend, Cat. #:318322), α-NKG2D (BioLegend, Cat. #:320820) and PE-conjugated goat anti-human IgG Fc secondary antibodies (Southern Biotech, Birmingham, USA).

Pharmocokinetics of IBI104

In a single-dose pharmacokinetics study, BALB/c mice were injected intravenously with IBI104 at a single dose of 10 mg/kg (3 males and 3 females in each group). Blood samples for PK analysis were drawn from all of the mice before dose administration and at 5 min; 2, 8 and 24 h; and 3, 7, 14, 21, 28, 35, 42 and 49 days post-dose administration, and processed for serum.

Statistical analysis

Statistical analyses were performed using GraphPad Prism (version 6.01 GraphPad Software Inc., San Diego, CA, USA). Statistical significance for tumor volume between the groups was determined using one-way ANOVA, and *P*-values <0.05 were considered to be statistically significant ($^{*}P \leq 0.05$, $^{**}P \leq 0.01$,$^{***}P \leq 0.001$ unless otherwise indicated in the figures).

SUPPLEMENTARY DATA

Supplementary Data are available at ABT Online.

ACKNOWLEDGEMENTS

The authors would like to thank Dr Siyi Hu and Li Li for their helpful suggestions on experiments.

AUTHOR CONTRIBUTIONS

Z.K. designed the study and performed the *in vitro* experiments; P.Z. performed the *in vivo* experiment; Li Li provided the hybridoma system; H.N. performed *in vitro* NK cell activation assay; B.C., M.W. and S.Y. assisted the *in vivo* experiment; J.Z. and Z.K. wrote the manuscript. All authors have read and approved the final manuscript.

CONFLICT OF INTEREST STATEMENT

All of the authors are employees of Innovent Biologics (Suzhou, China).

ETHICAL APPROVAL AND ETHICAL STANDARDS

All mice experiments were performed in accordance with regulations for the use of laboratory animals at Innovent Biologics and were approved by the Institutional Animal Care and Use Committee (IACUC-01).

REFERENCES

1. Ngiow, SF, von Scheidt, B, Akiba, H *et al.* Anti-TIM3 antibody promotes T cell IFN-gamma-mediated antitumor immunity and suppresses established tumors. *Cancer Res* 2011; **71**: 3540–51.
2. Dardalhon, V, Anderson, AC, Karman, J *et al.* Tim-3/galectin-9 pathway: regulation of Th1 immunity through promotion of CD11b+Ly-6G+ myeloid cells. *J Immunol* 2010; **185**: 1383–92.
3. Fourcade, J, Sun, Z, Benallaoua, M *et al.* Upregulation of Tim-3 and PD-1 expression is associated with tumor antigen-specific CD8+ T cell dysfunction in melanoma patients. *J Exp Med* 2010; **207**: 2175–86.
4. Koyama, S, Akbay, EA, Li, YY *et al.* Adaptive resistance to therapeutic PD-1 blockade is associated with upregulation of alternative immune checkpoints. *Nat Commun* 2016; **7**: 10501.
5. Shayan, G, Srivastava, R, Li, J *et al.* Adaptive resistance to anti-PD1 therapy by Tim-3 upregulation is mediated by the PI3K-Akt pathway in head and neck cancer. *Onco Targets Ther* 2017; **6**: e1261779.
6. Zhu, C, Anderson, AC, Schubart, A *et al.* The Tim-3 ligand galectin-9 negatively regulates T helper type 1 immunity. *Nat Immunol* 2005; **6**: 1245–52.
7. Cao, E, Zang, X, Ramagopal, UA *et al.* T cell immunoglobulin mucin-3 crystal structure reveals a galectin-9-independent ligand-binding surface. *Immunity* 2007; **26**: 311–21.
8. Santiago, C, Ballesteros, A, Tami, C *et al.* Structures of T cell immunoglobulin mucin receptors 1 and 2 reveal mechanisms for regulation of immune responses by the TIM receptor family. *Immunity* 2007; **26**: 299–310.
9. Chiba, S, Baghdadi, M, Akiba, H *et al.* Tumor-infiltrating DCs suppress nucleic acid-mediated innate immune responses through interactions between the receptor TIM-3 and the alarmin HMGB1. *Nat Immunol* 2012; **13**: 832–42.
10. Huang, YH, Zhu, C, Kondo, Y *et al.* CEACAM1 regulates TIM-3-mediated tolerance and exhaustion. *Nature* 2015; **517**: 386–90.
11. DeKruyff, RH, Bu, X, Ballesteros, A *et al.* T cell/transmembrane, Ig, and mucin-3 allelic variants differentially recognize phosphatidylserine and mediate phagocytosis of apoptotic cells. *J Immunol* 2010; **184**: 1918–30.
12. Seo, H, Jeon, I, Kim, BS *et al.* IL-21-mediated reversal of NK cell exhaustion facilitates anti-tumour immunity in MHC class I-deficient tumours. *Nat Commun* 2017; **8**: 15776.
13. Zhu, C, Sakuishi, K, Xiao, S *et al.* An IL-27/NFIL3 signalling axis drives Tim-3 and IL-10 expression and T-cell dysfunction. *Nat Commun* 2015; **6**: 6072.
14. Clayton, KL, Haaland, MS, Douglas-Vail, MB *et al.* T cell Ig and mucin domain-containing protein 3 is recruited to the immune synapse, disrupts stable synapse formation, and associates with receptor phosphatases. *J Immunol* 2014; **192**: 782–91.
15. Rangachari, M, Zhu, C, Sakuishi, K *et al.* Bat3 promotes T cell responses and autoimmunity by repressing Tim-3-mediated cell death and exhaustion. *Nat Med* 2012; **18**: 1394–400.
16. da Silva, IP, Gallois, A, Jimenez-Baranda, S *et al.* Reversal of NK-cell exhaustion in advanced melanoma by Tim-3 blockade. *Cancer Immunol Res* 2014; **2**: 410–22.
17. Pesce, S, Greppi, M, Tabellini, G *et al.* Identification of a subset of human natural killer cells expressing high levels of programmed death 1: a phenotypic and functional characterization. *J Allergy Clin Immunol* 2017; **139**: 335–46 e3.
18. Khademi, M, Illes, Z, Gielen, AW *et al.* T cell Ig- and mucin-domain-containing molecule-3 (TIM-3) and TIM-1 molecules

are differentially expressed on human Th1 and Th2 cells and in cerebrospinal fluid-derived mononuclear cells in multiple sclerosis. *J Immunol* 2004; **172**: 7169–76.
19. Barry, KC, Hsu, J, Broz, ML *et al.* A natural killer-dendritic cell axis defines checkpoint therapy-responsive tumor microenvironments. *Nat Med* 2018; **24**: 1178–91.
20. Anderson, AC, Anderson, DE, Bregoli, L *et al.* Promotion of tissue inflammation by the immune receptor Tim-3 expressed on innate immune cells. *Science* 2007; **318**: 1141–3.
21. Zhang, Y, Ma, CJ, Wang, JM *et al.* Tim-3 negatively regulates IL-12 expression by monocytes in HCV infection. *PLoS One* 2011; **6**: e19664.
22. Kobayashi, N, Karisola, P, Pena-Cruz, V *et al.* TIM-1 and TIM-4 glycoproteins bind phosphatidylserine and mediate uptake of apoptotic cells. *Immunity* 2007; **27**: 927–40.
23. Wong, K, Valdez, PA, Tan, C *et al.* Phosphatidylserine receptor Tim-4 is essential for the maintenance of the homeostatic state of resident peritoneal macrophages. *Proc Natl Acad Sci U S A* 2010; **107**: 8712–7.
24. Miyanishi, M, Tada, K, Koike, M *et al.* Identification of Tim4 as a phosphatidylserine receptor. *Nature* 2007; **450**: 435–9.
25. Patel, J, Bozeman, EN, Selvaraj, P. Taming dendritic cells with TIM-3: another immunosuppressive strategy used by tumors. *Immunotherapy* 2012; **4**: 1795–8.